

Transformation of spin current by antiferromagnetic insulators

Roman Khymyn,^{1,*} Ivan Lisenkov,^{1,2} Vasil S. Tiberkevich,¹ Andrei N. Slavin,¹ and Boris A. Ivanov^{3,4}

¹*Department of Physics, Oakland University, Rochester, Michigan 48309, USA*

²*Institute of Radio-engineering and Electronics of RAS, Moscow 125009, Russia*

³*Institute of Magnetism, NASU and MESYSU, Kiev 03142, Ukraine*

⁴*Taras Shevchenko National University of Kiev, 01601 Kiev, Ukraine*

(Received 29 November 2015; revised manuscript received 19 May 2016; published 22 June 2016)

It is demonstrated theoretically that a thin layer of an anisotropic antiferromagnetic (AFM) insulator can effectively conduct spin current through the excitation of a pair of evanescent AFM spin wave modes. The spin current flowing through the AFM is not conserved due to the interaction between the excited AFM modes and the AFM lattice and, depending on the excitation conditions, can be either attenuated or enhanced. When the phase difference between the excited evanescent modes is close to $\pi/2$, there is an optimum AFM thickness for which the output spin current reaches a maximum, which can significantly exceed the magnitude of the input spin current. The spin current transfer through the AFM depends on the ambient temperature and increases substantially when temperature approaches the Néel temperature of the AFM layer.

DOI: [10.1103/PhysRevB.93.224421](https://doi.org/10.1103/PhysRevB.93.224421)

I. INTRODUCTION

Progress in modern spintronics critically depends on finding novel media that can serve as effective conduits of spin angular momentum over large distances with minimum losses [1–3]. The mechanism of spin transfer is reasonably well understood in ferromagnetic (FM) metals [4,5] and insulators [3,4,6–9], but there are very few theoretical papers describing spin current in antiferromagnets (AFMs) (see, e.g., [10]).

Recent experiments [11–13] have demonstrated that a thin layer of a dielectric AFM (NiO, CoO) could effectively conduct spin current. The transfer of spin current was studied in the FM/AFM/Pt trilayer structure (see Fig. 1). The FM layer driven in ferromagnetic resonance (FMR) excited spin current in a thin layer of AFM, which was detected in the adjacent Pt film using the inverse spin Hall effect (ISHE). It was also found in [13] that the spin current through the AFM depends on the ambient temperature and goes through a maximum near the Néel temperature T_N . The most intriguing feature of the experiments was the fact that for a certain optimum thickness of the AFM layer (~ 5 nm) the detected spin current had a maximum [11,12], which could be even higher than in the absence of the AFM spacer [12]. The spin current transfer in the reversed geometry, when the spin current flows from the Pt layer driven by dc current through the AFM spacer into a microwave-driven FM material, has been reported recently in [14].

The experiments [11–14] posed a fundamental question of the mechanism of the apparently rather effective spin current transfer through an AFM dielectric. A possible mechanism of the spin transfer through an *easy-axis* AFM has been recently proposed in [10]. However, this uniaxial model cannot explain the nonmonotonic dependence of the transmitted spin current on the AFM layer thickness and the apparent “amplification” of the spin current seen in the experiments [11,12] performed with the *biaxial* NiO AFM layer [15].

In our current work, we propose a possible mechanism of spin current transfer through anisotropic AFM dielectrics, which may explain all the peculiarities of the experiments [11,12,14]. Namely, we show that the spin current can be effectively carried by the driven *evanescent* spin wave excitations, having frequencies that are much lower than the frequency of the AFM resonance. We demonstrate that the angular momentum exchange between the spin subsystem and the AFM lattice plays a crucial role in the process of spin current transfer, and may lead to the *enhancement* of the spin current by the angular momentum influx from the crystal lattice of the AFM.

II. SPIN DYNAMICS IN THE AFM DIELECTRICS

We consider a model of a simple AFM having two magnetic sublattices with the partial saturation magnetization M_s . The distribution of the magnetizations of each sublattice can be described by the vectors \mathbf{M}_1 and \mathbf{M}_2 , $|\mathbf{M}_1| = |\mathbf{M}_2| = M_s$. We use a conventional approach for describing the AFM dynamics by introducing the vectors of antiferromagnetism (\mathbf{l}) and magnetism (\mathbf{m}) [16–19]:

$$\mathbf{l} = (\mathbf{M}_1 - \mathbf{M}_2)/(2M_s), \quad \mathbf{m} = (\mathbf{M}_1 + \mathbf{M}_2)/(2M_s). \quad (1)$$

Assuming that all the magnetic fields are smaller than the exchange field H_{ex} and neglecting the bias magnetic field, which is used to saturate the FM layer, the effective AFM Lagrangian can be written as [16,18,19]

$$\mathcal{L} = \mu[(\partial\mathbf{l}/\partial t)^2 - c^2(\partial\mathbf{l}/\partial y)^2] - W_a - W_s\delta(y). \quad (2)$$

Here $\mu = M_s/(\gamma^2 H_{ex})$, γ is the gyromagnetic ratio, c is the speed of the AFM spin waves ($c \simeq 33$ km/s in NiO), and $W_a = M_s \mathbf{l} \cdot (\hat{\mathbf{H}}^a \cdot \mathbf{l})$ is the energy of the anisotropy, defined by the matrix of the anisotropy fields $\hat{\mathbf{H}}^a = \text{diag}(H_1^a, H_2^a, 0)$ with the diagonal (j, j) components $H_j^a = 2M_s\beta_j$ (β_j is the anisotropy constant along the j th axis). The equilibrium direction of the AFM vector $\mathbf{l}_0 = \mathbf{e}_3$ lies along the \mathbf{e}_3 axis.

The exchange coupling between the FM and AFM layers is modeled in Eq. (2) by the surface energy term $W_s = E_s[(\mathbf{m}_{\text{FM}} \cdot \mathbf{m}) + \alpha(\mathbf{m}_{\text{FM}} \cdot \mathbf{l})]$, where E_s is the surface

*khiminr@gmail.com

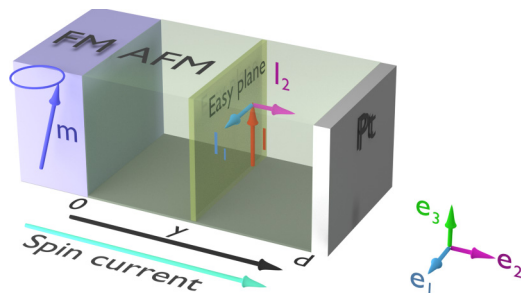


FIG. 1. Sketch of the model of spin current transfer through an AFM insulator based on the experiment [11]. The FM layer excites spin wave excitations in the AFM layer. The output spin current (at the AFM/Pt interface) is detected by the Pt layer through the inverse spin Hall effect (ISHE).

energy density and \mathbf{m}_{FM} is the unit vector of FM layer magnetization. We assumed that the net magnetization of the AFM at the FM/AFM interface layer could be partially noncompensated, and this “noncompensation” is characterized by a dimensionless parameter α ($0 < \alpha < 1$); see also the Appendix.

The dynamical equation for the AFM vector \mathbf{I} follows from the Lagrangian Eq. (2) and can be written as

$$\partial^2 \mathbf{I} / \partial t^2 + \Delta \omega \partial \mathbf{I} / \partial t - c^2 \partial^2 \mathbf{I} / \partial y^2 + \hat{\Omega} \cdot \mathbf{I} = \mathbf{f}(t) \delta(y), \quad (3)$$

where $\Delta \omega$ is the phenomenological damping parameter equal to the AFM resonance linewidth ($\Delta \omega / 2\pi \approx 69$ GHz for NiO [20]). Note that the damping-related decay length $\lambda_G = 2c / \Delta \omega \approx 150$ nm is much larger than the typical AFM thickness. Therefore, below we shall neglect damping except in Fig. 4, where the comparison of AFM spin currents in conservative and damped cases is presented. The matrix $\hat{\Omega} = \text{diag}(\omega_1^2, \omega_2^2, 0)$, and $\omega_j = \gamma \sqrt{H_{\text{ex}} H_j^a}$, $j = 1, 2$, are the frequencies of the AFM resonance. In the case of NiO the two AFM resonance frequencies are substantially different: $\omega_1 / 2\pi \simeq 240$ GHz and $\omega_2 / 2\pi \simeq 1.1$ THz [15]. We shall show below that the difference between the AFM resonance frequencies is crucially important for the spin current transfer through the AFM.

The driving force in Eq. (3) $\mathbf{f}(t) = -(\delta W_s / \delta \mathbf{I}) / (2\mu)$, localized at the FM/AFM interface, describes AFM excitation by the precessing FM magnetization. In the absence of this term Eq. (3) describes two branches of the eigenexcitations of the AFM with dispersion relations $\omega_j(\mathbf{k}) = \sqrt{\omega_j^2 + c^2 k^2}$. These propagating AFM spin waves have minimum frequencies ω_j which are much higher than the excitation frequency (9.65 GHz in Ref. [11]) and, therefore, cannot be responsible for the spin current transfer.

The presence of the FM layer, however, qualitatively changes the situation, as the driving force $\mathbf{f}(t)$ excites *evanescent* AFM spin wave modes at the frequency of the FM layer resonance (FMR), which is well below any of the AFMR frequencies ω_j . The profiles of the evanescent AFM modes can be easily found from Eq. (3):

$$\mathbf{I}_j(t, y) = \mathbf{e}_j [A_j e^{-y/\lambda_j} + B_j e^{y/\lambda_j}] e^{-i\omega t} + \text{c.c.}, \quad j = 1, 2, \quad (4)$$

where ω is the excitation frequency,

$$\lambda_j = c / \sqrt{\omega_j^2 - \omega^2} \quad (5)$$

is the penetration depth for the j th evanescent mode, and complex coefficients A_j, B_j are determined by the boundary conditions at the FM/AFM and AFM/Pt interfaces. The interfacial driving force $\mathbf{f}(t)\delta(y)$ excites the AFM vector $\mathbf{I}(t, y = 0)$ at the FM/AFM interface:

$$\mathbf{I}(t, y = 0) = \mathbf{e}_3 + [(a_1 \mathbf{e}_1 + a_2 \mathbf{e}_2) e^{-i\omega t} + \text{c.c.}]. \quad (6)$$

The complex amplitudes a_1 and a_2 depend on the vector structure of the magnetization precession in the FM layer (see Appendix for details), which opens a way to experimentally control the input spin current in the AFM, and to directly verify our theoretical predictions. Thus, if the FM layer is magnetized along one of the AFM anisotropy axes $\mathbf{e}_{1,2}$, the microwave magnetization component along that axis will be zero and the corresponding complex amplitude $a_{1,2}$ in Eq. (6) will vanish. On the other hand, if the FM layer is magnetized along the AFM equilibrium axis \mathbf{e}_3 , both amplitudes a_1 and a_2 will be nonzero with the phase shift $\phi = \arg(a_1/a_2) \approx \pi/2$ between them.

III. SPIN CURRENT THROUGH THE AFM LAYER

At the AFM/Pt interface ($y = d$) we adopt a simple form of the boundary conditions that were used previously for the description of spin current at the AFM/Pt [21] and FM/Pt [22] interfaces:

$$P(y = d) = \beta c L(y = d), \quad (7)$$

where P is the current of the \mathbf{e}_3 component of the spin angular momentum and L is the corresponding angular momentum density inside the AFM:

$$P = 2\mu c^2 \mathbf{e}_3 \cdot [\partial \mathbf{I} / \partial y \times \mathbf{I}], \quad L = -2M_s \gamma^{-1} \mathbf{e}_3 \cdot \mathbf{m}, \quad (8)$$

and β is a dimensionless constant having magnitude in the range from 0 to 1 and being physically determined by the spin mixing conductance at the AFM/Pt interface [22]. The case $\beta = 0$ corresponds to the conservative situation of a complete absence of the angular momentum flux, while the case $\beta = 1$ describes a “transparent” boundary, when the angular momentum freely moves across the AFM/Pt boundary without any reflection.

Using Eqs. (8), the boundary conditions Eq. (7) can be rewritten as explicit conditions on the vector of antiferromagnetism \mathbf{I} as $\beta \partial \mathbf{I} / \partial t = -c \partial \mathbf{I} / \partial y$. This equation and Eq. (6) allow one to find all four coefficients A_j, B_j in Eq. (4), and one can find the explicit expression for the spin current $P(y)$ inside the AFM layer:

$$P(y) = 4\mu c^2 |a_1 a_2| \text{Re}[Q(y) e^{-i\phi}], \quad (9)$$

where

$$Q(y) = \frac{(e^{-y/\lambda_1} + q_1 e^{y/\lambda_1})(e^{-y/\lambda_2} - q_2^* e^{y/\lambda_2})}{(1 + q_1)(1 + q_2^*)\lambda_2} - \frac{(e^{-y/\lambda_1} - q_1 e^{y/\lambda_1})(e^{-y/\lambda_2} + q_2^* e^{y/\lambda_2})}{(1 + q_1)(1 + q_2^*)\lambda_1}. \quad (10)$$

Here $q_j = e^{2i\psi_j - 2d/\lambda_j}$ and $\psi_j = \arctan(\beta\omega\lambda_j/c) \approx \beta\omega/\omega_j$. Equation (9) is the central result of this paper that allows one to find the spin current carried by the evanescent spin wave modes in an AFM layer.

Now we shall analyze the main features of the spin current transfer through an AFM dielectric that are described by Eq. (9). First, one can see that the spin current P is proportional to the product $|a_1 a_2|$ of the amplitudes of both excited evanescent spin wave modes, and this current is completely absent if only one of the modes is excited. This is explained by the fact that each of the modes Eq. (4) is linearly polarized, and, therefore, cannot alone carry any angular momentum.

Second, the spin current in the AFM layer depends on the position y inside the AFM layer; i.e., it is *not conserved*. This is a direct consequence of the assumed biaxial anisotropy of the AFM material, which allows for the transfer of the angular momentum between the spin subsystem and the crystal lattice of the AFM layer. This effect is a magnetic analog of the optical effect of birefringence [23], where the spin angular momentum of light is dynamically changed during its propagation in a birefringent medium.

In the case of a uniaxial anisotropy [10] ($\lambda_1 = \lambda_2 = \lambda$) Eq. (9) can be simplified to

$$P = \frac{16\mu c^2}{\lambda} \frac{\text{Im}(q)}{|1+q|^2} |a_1 a_2| \sin \phi, \quad (11)$$

and the spin current is *conserved* across the whole AFM layer.

Equation (9) can also be simplified in the case of a semi-infinite AFM layer, in which case $\mathcal{B}_j = 0$ and $q_1 = q_2 = 0$:

$$P = \frac{4\mu c^2(\lambda_1 - \lambda_2)}{\lambda_1 \lambda_2} |a_1 a_2| \cos \phi e^{-y/\lambda_{\text{eff}}}. \quad (12)$$

In such a case the spin current decays monotonically inside the AFM layer with the effective penetration depth $\lambda_{\text{eff}} = \lambda_1 \lambda_2 / (\lambda_1 + \lambda_2) \simeq 5$ nm for NiO.

Another peculiarity of Eq. (9) and Eq. (11) is that the spin current P depends on the phase shift ϕ between the two excited evanescent AFM spin wave modes \mathbf{I}_1 and \mathbf{I}_2 :

$$P \propto \cos[\phi - \Phi(y)], \quad (13)$$

where $\Phi(y) = \arg[Q(y)]$. The maximum spin current at a given position y inside the AFM layer is achieved at $\phi = \Phi(y)$. Since the AFM phase shift $\Phi(y)$, in general, depends on the position y inside the AFM layer, for any particular thickness d of the AFM layer it is possible to choose the excitation phase shift ϕ that would maximize the output spin current $P(y = d)$, while the input spin current $P(y \rightarrow 0)$ could be quite low. In such a case the additional angular momentum is taken from the crystal lattice of the AFM. This shows that, in principle, the AFM dielectrics can serve as “amplifiers” of a spin current.

Figure 2 shows the spatial profiles of the spin current density in a relatively thick AFM layer (thickness $d = 20$ nm). This dependence is drastically different for different phase shifts ϕ between the excited evanescent spin wave modes. While for $\phi < \pi/2$ the spin current exponentially and monotonically decays inside the AFM layer (dashed blue line in Fig. 2), for $\phi > \pi/2$ (solid black line in Fig. 2) it initially increases at relatively small y due to the angular momentum flow from the AFM crystal lattice to its spin subsystem. At larger values of

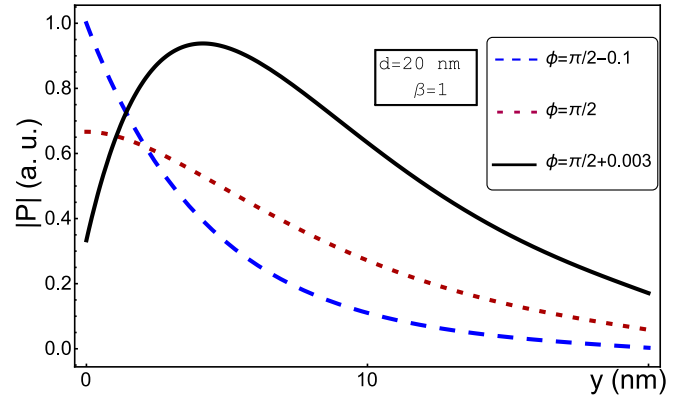


FIG. 2. Spatial distribution of the spin current $P(y)$ inside the AFM layer for different phase shifts ϕ between the two evanescent AFM spin wave modes calculated from Eq. (9).

y , the spin current decays exponentially due to the decay of the excited evanescent spin wave modes.

Figure 3 demonstrates the dependencies of the spin current on the phase shift ϕ at both interfaces FM/AFM (input spin current) and AFM/Pt (output spin current). It is clear from Fig. 3 that the output spin current is shifted by $\sim \pi/2$ relative to the input spin current, and, for the phase shift $\phi \approx \pi/2$, the output spin current could have a maximum magnitude when the input spin current is almost completely absent. This means that at such a value of the phase shift between the evanescent spin wave modes practically all the output spin current is generated as a result of interaction between the magnetic subsystem of the AFM layer and its crystal lattice. Thus, the AFM layer acts as a *source* of the spin current. On the other hand, at the phase shift of $\phi \approx 0$ or $\phi \approx \pi$, the situation is opposite, as the input spin current is practically lost inside the AFM, and the AFM layer acts as a spin current *sink*.

Thus, we showed that a thin layer of AFM, driven by a constant flow of microwave energy from the FM layer, is able to transform the angular momentum of a crystal lattice into the spin current and vice versa. The described transfer of the angular momentum from the lattice to the spin system has a simple analog not only as a birefringence in optics, but also in mechanics: a mechanical oscillator which consists of a mass

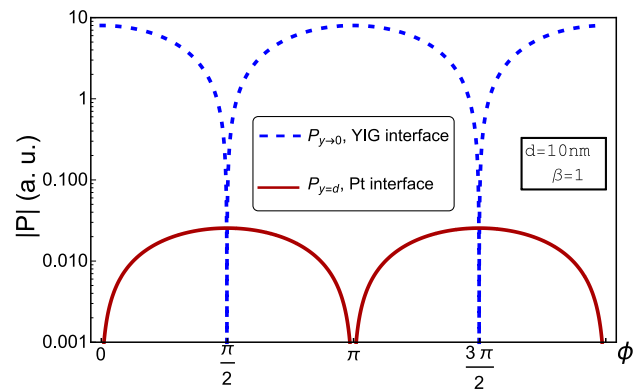


FIG. 3. Dependence of the input (dashed blue line) and output (solid red line) spin currents through the AFM layer on the phase shift ϕ between the modes.

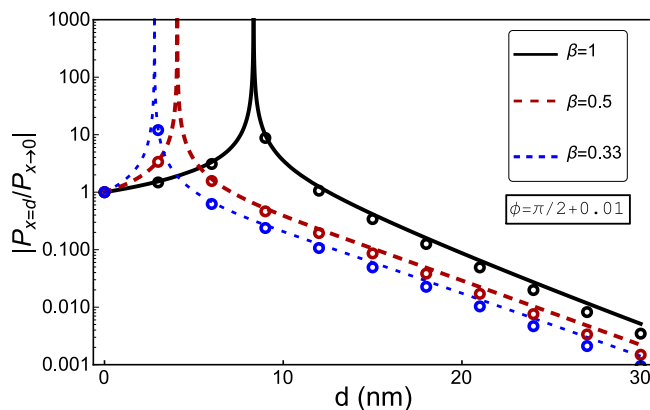


FIG. 4. Spin current transfer factor of the AFM layer as a function of the AFM layer thickness for different values of the spin mixing conductance parameter β . The lines show the case of zero damping ($\Delta\omega = 0$), while the circles correspond to the AFMR linewidth of $\Delta\omega/2\pi = 69$ GHz [20].

suspended on two perpendicular springs with different stiffness attached to a fixed rectangular frame. The displacement of the mass from its equilibrium position in the frame center along the direction of one of the orthogonal springs results in the linearly polarized oscillations along this direction, without any transfer of the angular momentum from the frame to the oscillating mass. In contrast, the linear displacement of the mass in a *diagonal* direction results in the *rotation* of the mass around its equilibrium position, and the angular momentum necessary for this rotation is taken from the frame (see animations in Supplemental Material [27]).

The ratio of the output spin current to the input one (the spin current transfer factor) is shown in Fig. 4 for different values of the constant β , i.e., for the different values of the spin mixing conductance at the AFM/Pt interface. This dependence has a sharp maximum at the thickness of a few nanometers, where the input current is rather low, and the AFM layer acts as a source of a spin current. With the further increase of the AFM layer thickness the transfer ratio is exponentially decreasing, while the position of the maximum shifts to the right with the increase of the spin mixing conductance at the AFM/Pt interface. As one can see from Fig. 4, the presence of the damping has little influence on the spin current, because the spatial decay of the amplitudes due to the evanescent character of the modes $\mathbf{I}_{1,2}$ is dominant.

IV. ENERGY EFFICIENCY OF THE SPIN TRANSFER

It is obvious that, besides the spin transfer through the AFM dielectric, there is also a *flux of energy* through the AFM layer. This flux of energy Π can be found from the Lagrangian Eq. (2) by applying the Noether theorem, and has the following form:

$$\Pi = 8 \frac{\mu c^3 \omega^2}{\beta} \sum_{i=1,2} \frac{a_i^2}{(c^2/\beta^2 - \omega^2 \lambda_i^2)(1 + \cosh 2d/\lambda_i)}. \quad (14)$$

As one can see from Eq. (14), the flux of energy does not depend on either the spatial coordinate y inside the AFM and the phase shift ϕ between the excited evanescent AFM modes.

Therefore, the FM layer is a source and the Pt layer is a receiver of the energy coming from the FM layer, and this flux of energy is not transformed inside the AFM layer (besides negligible Gilbert damping; see Fig. 4).

At the same time, the situation with the spin current is quite different. Due to the anisotropy of the AFM layer the angular momentum is not conserved inside the magnetic subsystem of the AFM layer, and, therefore, there appears a flux of angular momentum between the spin subsystem and the lattice of the AFM.

Therefore, as was discussed above, at certain parameters of the spin dynamics in the AFM it is possible to create a flux of angular momentum from the lattice into the spin subsystem. In this case it is possible to get the output spin current that is larger than the input one, but, obviously, the flux of energy at the output will never be larger than at the input.

The efficiency of the spin transfer through the AFM layer can be characterized by the ratio of the spin current at the output of the AFM layer to the energy losses of the FM layer. Thus, we can introduce the value $S_{\text{eff}} = \omega P|_{y=d}/\Pi$, which is defined as the ratio of the transferred angular momentum to the energy flux, and, therefore, can be interpreted as “effective spin” of the spin transfer.

As one can see, the energy flux is the sum of the energies of both evanescent AFM modes, and has the form $\Pi = A_1 a_1^2 + A_2 a_2^2$, while the spin current depends on the product of the modes’ amplitudes $P = C|a_1 a_2|$. Thus, the effective spin has a maximum, and the value of this maximum is $S_{\text{eff}} = C/2\sqrt{A_1 A_2}$. Maximizing this value with respect to the phase shift ϕ between the excited evanescent AFM modes one can obtain the maximum efficiency of the spin transfer $S_{\text{eff}}^{\text{max}} = 1$, which is the same as for propagating spin waves in ferromagnetic materials.

Physically, the difference in the behavior of the energy and the spin flux originates from the symmetries of the Lagrangian (2). The flux of energy is defined by the infinitesimal shifts of the Lagrangian in *time*, which are symmetric in the absence of damping, resulting in the energy conservation. In contrast, the flux of the angular momentum is determined by the infinitesimal *rotations* of the Lagrangian (2). Obviously, the operation of rotation does not transform the system to itself in the case of a biaxial anisotropy, and, therefore, the angular momentum in the spin system of an anisotropic AFM is not conserved.

V. ISHE VOLTAGE IN PT LAYER

Using Eq. (9), we estimated the ISHE voltage for an FM/AFM/Pt structure (and, in particular, for the NiFe/NiO/Pt structure) with the AFM layer having thickness d , which is smaller than the penetration depths λ_j of both evanescent AFM modes. To find the amplitudes a_1 and a_2 of the evanescent modes, we adopt a simple model, where we assume that the precession of the magnetization in the FM layer excites spin dynamics of the AFM; see the Appendix. Following [24], the ISHE voltage can be written as

$$V_{\text{ISHE}} = \rho_{\Theta SH} w \left(\frac{2e}{\hbar} \right) \frac{\lambda_{Pt}}{d_{Pt}} \tanh \left(\frac{d_{Pt}}{2\lambda_{Pt}} \right) P_d, \quad (15)$$

where ρ is the resistivity of the Pt, $w = 5$ nm is the distance between the probe electrodes attached to the Pt layer, $d_{Pt} = 10$ nm is the thickness of the Pt layer, $\Theta_{SH} = 0.05$ is the spin Hall angle in Pt, $\lambda_{Pt} = 7.7$ nm is the spin diffusion length in Pt, e is the electron charge, and \hbar is the Planck constant.

It is important to note that the value of the interface exchange integral J_s and, correspondingly, the value of the surface energy density E_s strongly depend on the method of fabrication of the sample, and, therefore, can be measured only in an experiment performed for a particular sample. To give a reasonable numerical example, below we take the value of E_s to be $E_s = 3.3 \times 10^{-3}$ J/m², which was measured for the NiFe/NiO interface in [25].

For the given parameters, taking the angle of magnetization precession in the FM layer, $\sin\theta = 0.01$ [see Eq. (A5)], we obtain $V_{ISHE} = 40$ mV for the *uncompensated* AFM boundary ($\alpha = 1$) and $V_{ISHE} = 4$ nV for the *compensated* one ($\alpha = 0$). The first value is close to the ISHE voltage measured in Ref. [11]. A partial interfacial magnetization of the antiferromagnetic NiO in that case was confirmed by the XRD scan performed in [11]. The calculated ISHE voltage for the compensated AFM is closer to the experimental value obtained in Ref. [12].

The reason for such a small magnitude of the ISHE voltage in the case of a *compensated* AFM interface is obvious. Since the dynamic magnetization \mathbf{m} in the “compensated” case is $\gamma H_{ex}/\omega$ times smaller than the magnitude of the AFM vector \mathbf{l} , the energy of the exchange coupling W_s at the FM/AFM interface in Eq. (2) is rather small.

VI. DISCUSSION

The above presented results were obtained for the parameters of a bulk NiO sample at low temperature. However, it is well known that such important parameters of AFM substances as the anisotropy constants and Néel temperature in thin AFM films could be substantially smaller than in bulk crystals (see, e.g., [26]). Thus, the penetration depths of the evanescent spin wave modes Eq. (5), determined at a given driving frequency ω by the AFM anisotropy constants, would significantly depend on the thickness and the temperature of the AFM layer. Particularly, with the increase of temperature the AFMR frequencies ω_j would decrease, and would approach zero at the Néel temperature [20]. In accordance with Eq. (5), this means that the penetration depth of the evanescent AFM spin wave modes will increase substantially when the temperature approaches the Néel temperature of the AFM layer. This increase of the spin current transferred through the AFM layer is clearly seen in the experiments [13].

In conclusion, we demonstrated that the spin current can be effectively transmitted through thin dielectric AFM layers by a pair of externally excited evanescent AFM spin wave modes. In the case of AFM materials with biaxial anisotropy the transfer of angular momentum between the spin subsystem and the crystal lattice of the AFM can lead to the enhancement or decrease of the transmitted spin current, depending on the phase relation between the excited evanescent spin wave modes. Our results explain all the qualitative features of the recent experiments [11–14], in particular, the existence of an optimum thickness of the AFM layer, for which the output

current could reach a maximum value which is higher than the spin current magnitude in the absence of the AFM spacer, and the increase of the transmitted spin current at the temperatures close to the Néel temperature of the AFM layer.

ACKNOWLEDGMENTS

This work was supported in part by Grant No. ECCS-1305586 from the National Science Foundation of the USA, by the contract from the US Army TARDEC, RDECOM, by DARPA MTO/MESO Grant No. N66001-11-4114, and by the Center for NanoFerroic Devices (CNFD) and the Nanoelectronics Research Initiative (NRI).

APPENDIX: AFM DYNAMICS DRIVEN BY THE MAGNETIZATION PRECESSION IN AND ADJACENT TO THE FM LAYER

Let us consider the excitation of dynamics in an AFM layer by the processes happening at the FM/AFM interface. Let us assume that the magnetic coupling between the FM and AFM is of the exchange origin and, therefore, is strongly localized at the AFM/FM interface. The spins existing at the AFM boundary can belong either to two different sublattices of the AFM, as shown in Fig. 5(a), or to the same sublattice [see Fig. 5(b)]. In the first case the AFM has no static magnetization at the interface and will be called below a *compensated* AFM, while in the second case, the boundary of the AFM is magnetized, and such AFM will be called *uncompensated*.

The exchange coupling between the FM and AFM layers creates an additional term in the energy of the AFM. In the case of a *compensated* AFM the additional energy is expressed as $\Delta E = \sum J_s (\tilde{\mathbf{S}} \cdot \mathbf{S}_1 + \tilde{\mathbf{S}} \cdot \mathbf{S}_2)$, where J_s is the interface exchange integral, $\tilde{\mathbf{S}}$ is the FM spin at the interface, and the summation is taken over the whole FM/AFM interface.

After the transition to a continuum limit and taking into account the relation Eq. (1) in the main text of the paper, one can write the additional term in the Lagrangian Eq. (2) as $E_s (\mathbf{m}_{FM} \cdot \mathbf{m}) \delta(y)$, where \mathbf{m}_{FM} is the unit vector defining the magnetization direction in the FM layer, E_s is the density of the surface exchange energy describing FM/AFM coupling, and E_s is proportional to the exchange integral J_s : $E_s \propto J_s$.

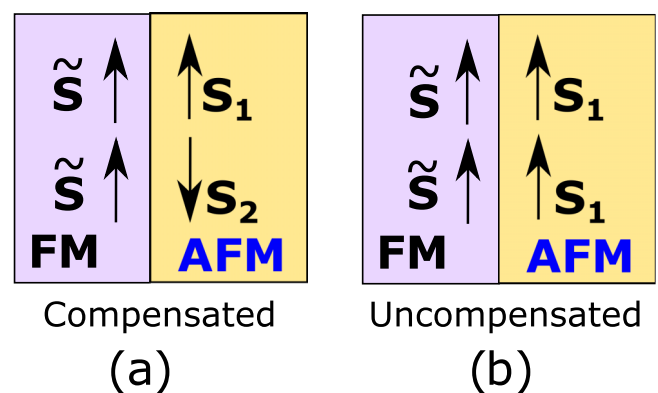


FIG. 5. Two types of FM/AFM interface: (a) totally compensated AFM boundary with zero magnetization, (b) totally uncompensated AFM boundary.

Considering the case of an *uncompensated* boundary of the AFM, one can find the additional coupling energy as $\Delta E = \sum 2J_s \mathbf{S} \cdot \mathbf{S}_1$, which leads to the term $E_s[\mathbf{m}_{\text{FM}} \cdot (\mathbf{m} + \mathbf{l})]\delta(y)$. Usually, the AFM boundary is *partially uncompensated*, and we introduce the phenomenological parameter $\alpha \in [0 \dots 1]$, which describes the *degree of the AFM noncompensation* at the FM/AFM interface.

Using the well-known expression for the AFM magnetization [16,18,19],

$$\mathbf{m} = \frac{1}{\gamma H_{ex}} \left[\mathbf{l} \times \frac{\partial \mathbf{l}}{\partial t} \right], \quad (\text{A1})$$

it is easy to obtain the Lagrange equations describing the spin dynamics inside the AFM:

$$2\mu \left\{ \left[\mathbf{l} \times \frac{\partial^2 \mathbf{l}}{\partial t^2} \right] - c^2 \left[\mathbf{l} \times \frac{\partial^2 \mathbf{l}}{\partial x^2} \right] \right\} - \left[\mathbf{l} \times \frac{\partial W_a}{\partial \mathbf{l}} \right] = E_s \delta(y) \left\{ \alpha [\mathbf{l} \times \mathbf{m}_{\text{FM}}] + \left[\mathbf{l} \times \frac{1}{\gamma H_{ex}} \left(2 \left[\frac{\partial \mathbf{l}}{\partial t} \times \mathbf{m}_{\text{FM}} \right] + \left[\mathbf{l} \times \frac{\partial \mathbf{m}_{\text{FM}}}{\partial t} \right] \right) \right] \right\}. \quad (\text{A2})$$

Since vector \mathbf{l} in the ground state is directed along the vector \mathbf{e}_3 , we can, in the case of a negligibly small dissipation, write the dynamic equations for only two components l_1 and l_2 of the vector \mathbf{l} . These equations have the form analogous to the form of the dynamic equation (3) in the main text of the paper:

$$\frac{\partial^2 l_1}{\partial t^2} - c^2 \frac{\partial^2 l_1}{\partial y^2} + \omega_1^2 l_1 = \frac{E_s \delta(y)}{2\mu} \left\{ \alpha (\mathbf{m}_{\text{FM}} \cdot \mathbf{e}_1) + \frac{1}{\gamma H_{ex}} \left[2 \frac{\partial l_2}{\partial t} (\mathbf{m}_{\text{FM}} \cdot \mathbf{l}) + l_2 \left(\frac{\partial \mathbf{m}_{\text{FM}}}{\partial t} \cdot \mathbf{l} \right) \right] - \left(\frac{\partial \mathbf{m}_{\text{FM}}}{\partial t} \cdot \mathbf{e}_2 \right) \right\}, \quad (\text{A3})$$

$$\frac{\partial^2 l_2}{\partial t^2} - c^2 \frac{\partial^2 l_2}{\partial y^2} + \omega_2^2 l_2 = \frac{E_s \delta(y)}{2\mu} \left\{ \alpha (\mathbf{m}_{\text{FM}} \cdot \mathbf{e}_2) - \frac{1}{\gamma H_{ex}} \left[2 \frac{\partial l_1}{\partial t} (\mathbf{m}_{\text{FM}} \cdot \mathbf{l}) + l_1 \left(\frac{\partial \mathbf{m}_{\text{FM}}}{\partial t} \cdot \mathbf{l} \right) \right] - \left(\frac{\partial \mathbf{m}_{\text{FM}}}{\partial t} \cdot \mathbf{e}_1 \right) \right\}. \quad (\text{A4})$$

The above equations are the equations describing dynamics of an oscillatory system driven by an external force $\mathbf{f}(t)\delta(y)$, where $\mathbf{f}(t)$ are the right-hand-side parts of the above equations.

We consider the harmonic driving force and, therefore, $\mathbf{m}_{\text{FM}} \propto e^{-i\omega t}$. In this case, when $\omega < \omega_1, \omega_2$ the solutions of these equations are the evanescent modes that exponentially decay with the increase of the coordinate y inside the AFM. These solutions are given explicitly by Eq. (4) in the main paper.

To obtain the values of the amplitudes a_1 and a_2 in Eq. (6) we consider a generic case, when the magnetization in the FM layer is parallel to the AFM vector $\mathbf{m}_{\text{FM}} = \mathbf{e}_3$. Then, the precessing magnetization in the FM layer can be expressed as

$$\begin{aligned} \mathbf{m}_{\text{FM}} \cdot \mathbf{e}_1 &= \sin \theta \sin \omega t, \\ \mathbf{m}_{\text{FM}} \cdot \mathbf{e}_2 &= \sin \theta \cos \omega t, \end{aligned} \quad (\text{A5})$$

where θ is the magnetization precession angle in the FM. In this case, the amplitudes a_1 and a_2 of the two evanescent modes l_1, l_2 have the form

$$|a_1| = \gamma \frac{E_s}{2M_s} \frac{|\omega + \alpha \gamma H_{ex}|}{c \sqrt{\omega_1^2 - \omega^2}} \sin \theta, \quad (\text{A6})$$

$$|a_2| = \gamma \frac{E_s}{2M_s} \frac{|-\omega + \alpha \gamma H_{ex}|}{c \sqrt{\omega_2^2 - \omega^2}} \sin \theta, \quad (\text{A7})$$

and the phase shift is $\phi = \pi/2$.

-
- [1] S. A. Wolf, D. D. Awschalom, R. A. Buhrman, J. M. Daughton, S. von Molnar, M. L. Roukes, A. Y. Chtchelkanova, and D. M. Treger, *Science* **294**, 1488 (2001).
- [2] S. Maekawa, *Concepts in Spin Electronics* (Oxford University Press, Oxford, UK, 2006), Chaps. 7 and 8.
- [3] V. E. Demidov, S. Urazhdin, H. Ulrichs, V. Tiberkevich, A. Slavin, D. Baither, G. Schmitz, and S. O. Demokritov, *Nat. Mater.* **11**, 1028 (2012).
- [4] Y. Kajiwara, K. Harii, S. Takahashi, J. Ohe, K. Uchida, M. Mizuguchi, H. Umezawa, H. Kawai, K. Ando, K. Takanashi, S. Maekawa, and E. Saitoh, *Nature (London)* **464**, 262 (2010).
- [5] T. Valet and A. Fert, *Phys. Rev. B* **48**, 7099 (1993).
- [6] J. E. Hirsch, *Phys. Rev. Lett.* **83**, 1834 (1999).
- [7] Z. Li and S. Zhang, *Phys. Rev. Lett.* **92**, 207203 (2004).
- [8] M. Tsoi, V. Tsoi, J. Bass, A. G. M. Jansen, and P. Wyder, *Phys. Rev. Lett.* **89**, 246803 (2002).
- [9] H. Kurebayashi, O. Dzyapko, V. E. Demidov, D. Fang, A. J. Ferguson, and S. O. Demokritov, *Nat. Mater.* **10**, 660 (2011).
- [10] S. Takei, T. Moriyama, T. Ono, and Y. Tserkovnyak, *Phys. Rev. B* **92**, 020409(R) (2015).
- [11] H. Wang, C. Du, P. C. Hammel, and F. Yang, *Phys. Rev. Lett.* **113**, 097202 (2014).
- [12] C. Hahn, G. de Loubens, V. V. Naletov, J. B. Youssef, O. Klein, and M. Viret, *Europhys. Lett.* **108**, 57005 (2014).
- [13] Z. Qiu, J. Li, D. Hou, E. Arenholz, A. T. NDiaye, A. Tan, K. Uchida, K. Sato, Y. Tserkovnyak, Z. Qiu, and E. Saitoh, *arXiv:1505.03926*.

- [14] T. Moriyama, S. Takei, M. Nagata, Y. Yoshimura, N. Matsuzaki, T. Terashima, Y. Tserkovnyak, and T. Ono, *Appl. Phys. Lett.* **106**, 162406 (2015).
- [15] M. T. Hutchings and E. J. Samuelsen, *Phys. Rev. B* **6**, 3447 (1972).
- [16] A. Andreev and V. Marchenko, *Sov. Phys. Usp.* **23**, 21 (1980).
- [17] I. Affleck and R. A. Weston, *Phys. Rev. B* **45**, 4667 (1992).
- [18] A. M. Kosevich, B. A. Ivanov, and A. S. Kovalev, *Phys. Rep.* **194**, 117 (1990).
- [19] T. Satoh, S.-J. Cho, R. Iida, T. Shimura, K. Kuroda, H. Ueda, Y. Ueda, B. A. Ivanov, F. Nori, and M. Fiebig, *Phys. Rev. Lett.* **105**, 077402 (2010).
- [20] A. J. Sievers and M. Tinkham, *Phys. Rev.* **129**, 1566 (1963).
- [21] R. Cheng, J. Xiao, Q. Niu, and A. Brataas, *Phys. Rev. Lett.* **113**, 057601 (2014).
- [22] Y. Tserkovnyak, A. Brataas, and G. E. W. Bauer, *Phys. Rev. Lett.* **88**, 117601 (2002).
- [23] M. Born and E. Wolf, *Principles of Optics: Electromagnetic Theory of Propagation, Interference, and Diffraction of Light* (Cambridge University Press, Cambridge, UK, 1997), Chap. 9.
- [24] H. Nakayama, K. Ando, K. Harii, T. Yoshino, R. Takahashi, Y. Kajiwara, K. Uchida, Y. Fujikawa, and E. Saitoh, *Phys. Rev. B* **85**, 144408 (2012).
- [25] B. K. Kuanr, R. E. Camley, and Z. Celinski, *J. Appl. Phys.* **93**, 7723 (2003).
- [26] D. Alders, L. H. Tjeng, F. C. Voogt, T. Hibma, G. A. Sawatzky, C. T. Chen, J. Vogel, M. Sacchi, and S. Iacobucci, *Phys. Rev. B* **57**, 11623 (1998).
- [27] See Supplemental Material at <http://link.aps.org/supplemental/10.1103/PhysRevB.93.224421> for animations of the mechanical oscillator with a mass on two orthogonal springs. Excitation along the direction of the spring and the excitation in the diagonal direction, which results in the rotation of the mass, are both shown.